Journal of Bioenergetics and Biomembranes, Vol. 30, No. 1, 1998

Crystal Structure of Bovine Heart Cytochrome *c* Oxidase at 2.8 Å Resolution

Shinya Yoshikawa,[1] Kyoko Shinzawa-Itoh,[1] and Tomitake Tsukihara[2]

Received September 22, 1997; accepted October 1, 1997

Thirteen different polypeptide subunits, each in one copy, five phosphatidyl ethanolamines and three phosphatidyl glycerols, two hemes A, three Cu ions, one Mg ion, and one Zn ion are detectable in the crystal structure of bovine heart cytochrome *c* oxidase in the fully oxidized form at 2.8 Å resolution. A propionate of hems *a*, a peptide unit (–CO–NH–), and an imidazole bound to Cu_A are hydrogen-bonded sequentially, giving a facile electron transfer path from Cu_A to heme *a*. The O_2 binding and reduction site, heme a_3, is 4.7 Å apart from Cu_B. Two possible proton transfer paths from the matrix side to the cytosolic side are located in subunit I, including hydrogen bonds and internal cavities likely to contain randomly oriented water molecules. Neither path includes the O_2 reduction site. The O_2 reduction site has a proton transfer path from the matrix side possibly for protons for producing water. The coordination geometry of Cu_B and the location of Tyr^{244} in subunit I at the end of the scalar proton path suggests a hydroperoxo species as the two electron reduced intermediate in the O_2 reduction process.

KEY WORDS: Cytochrome *c* oxidase; membrane protein; proton pump; O_2 reduction; x-ray crystal structure.

INTRODUCTION

Bovine heart cytochrome *c* oxidase is the largest and one of the most extensively investigated terminal oxidases (Malmström, 1990; Calhoun *et al.*, 1994; Ferguson-Miller and Babcock, 1996). Before the crystal structure appeared, 13 different polypeptide subunits (Kadenbach *et al.*, 1983) and redox-inactive metals, Mg and Zn besides Fe and Cu (Einarsdottir and Caughey, 1985; Steffens *et al.*, 1987), had been proposed as the intrinsic constituents of bovine heart enzyme. A bacterial cytochrome *c* oxidase preparation containing only subunits I and II reduces O_2 by the electrons from cytochrome *c* coupled with proton pumping (Hendler *et al.*, 1991). Thus, the physiological roles of another 11 subunits as well as the two redox inactive metals are intriguing subjects to investigate. The crystal structure of eukaryotic cytochrome *c* oxidase at atomic resolution is indispensable for such an investigation, as well as for understanding the mechanism of redox-coupled proton pumping.

Here we discuss the crystal structure of the oxidized bovine heart cytochrome *c* oxidase at 2.8 Å resolution and its functional implications.

PROTEIN STRUCTURE

The 13 subunits, each in one copy, are located in the crystal structure of bovine heart cytochrome *c* oxidase as shown in Fig. 1 (Tsukihara *et al.*, 1996). The enzyme is in a dimer state in this crystal. The middle portion of the crystal structure is a large bundle of 28 α-helices, 50 Å in length. Thus, the bundle is assignable to the transmembrane moiety in the mitochondrial inner membrane. The Cu_A site, which contains two copper atoms, is located in an extramembrane

[1] Department of Life Science, Himeji Institute of Technology, Kamigohri, Akoh Hyogo 678-12, Japan.
[2] Institute for Protein Research, Osaka University, Suita, Osaka 565, Japan.

0145-479X/98/0200-0007$15.00/0

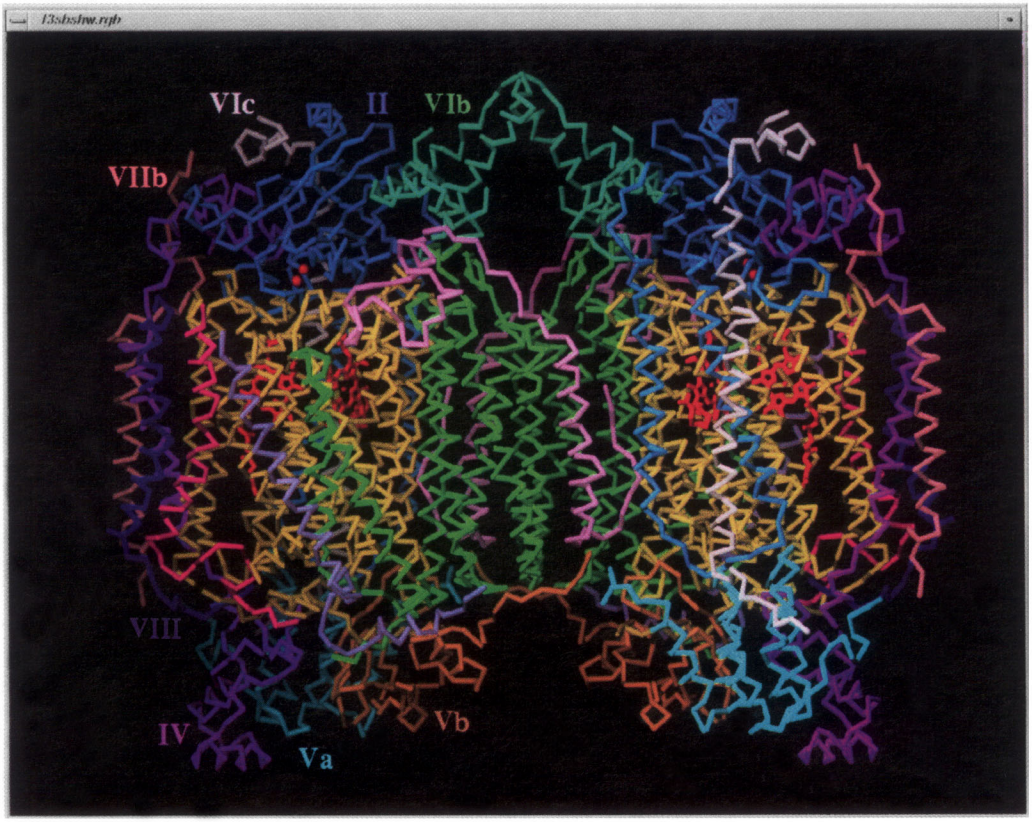
VIc
II
VIb
VIIb
VIII
IV
Va
Vb

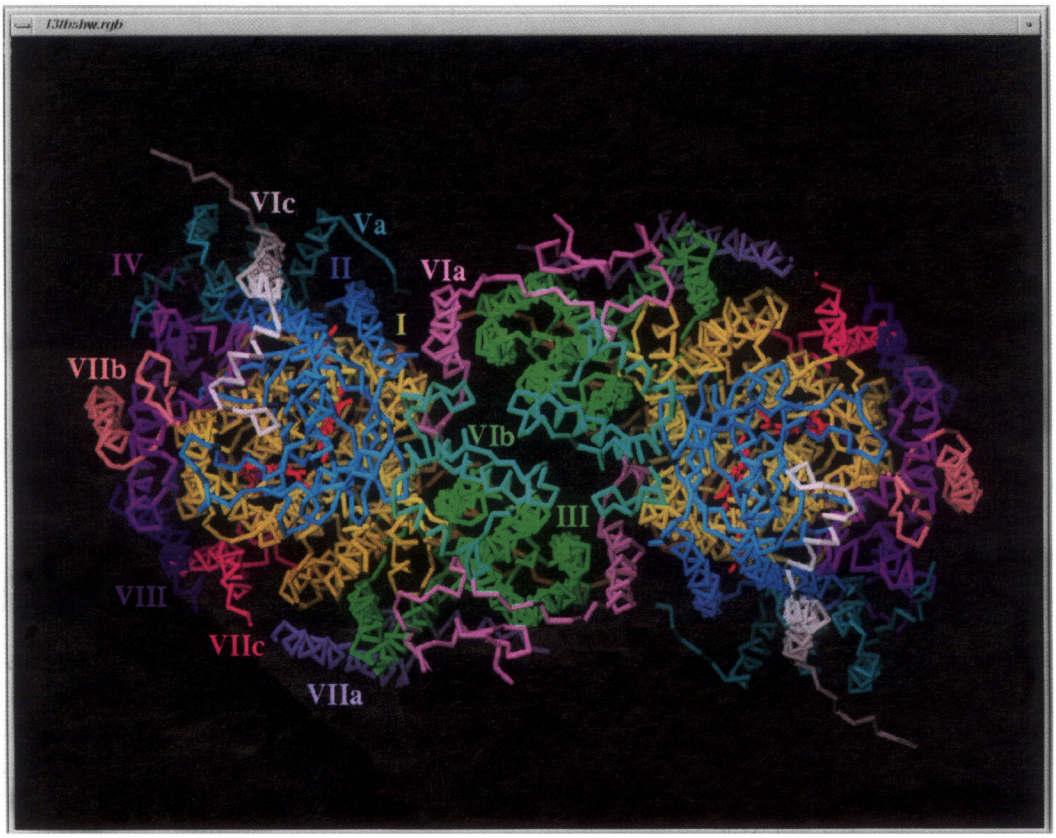
VIc
Va
IV
II
VIa
I
VIIb
VIb
III
VIII
VIIc
VIIa

domain, and identifies the cytosolic side. Thus zinc is in the extramembrane domain on the matrix side (Fig. 1). The transmembrane helix regions in the largest three subunits (subunits I, II, and III; encoded by mitochondrial genes) were fairly well predicted by the amino acid sequences (Capaldi, 1990). However, most of the helix regions in the crystal structure are longer than predicted (Tsukihara *et al.*, 1996). The prediction seems much less reliable in the region containing metal sites. For example, the segment including two histidines bound to Cu_B, His^{290}, and His^{291}, between helices VII and VIII, was predicted to be a part of a transmembrane α helix region.

POSSIBLE ROLES OF SUBUNITS WHICH DO NOT CONTAIN REDOX ACTIVE METALS

The three-dimensional structure suggests some physiological roles for subunits other than subunits I and II. Most of the transmembrane helices are placed not completely perpendicularly to the membrane surface, but at angles of 20° to 35° from the membrane normal. Any one of a pair of nearest neighbor helices in our crystal structure crosses with the other in three types of most stable helix–helix interactions, that is, with crossing angles of approximately O°, 20°, and 50° (Chotia *et al.*, 1977). These helix–helix contacts may contribute to the stability of the enzyme. Seven nuclear-coded subunits, each with a single transmembrane α helix, surrounds the largest three core subunits (subunits I, II, and III) (Fig. 2). Thus, a role of these nuclear subunits may be to promote the conformational stability of the core subunits.

The second largest subunit, subunit III, holds a phosphatidylglycerol and two phosphatidylethanolamine molecules in a large cleft to place the phospholipid cluster on the entrance of one of the three possible O_2 channels to the O_2 reduction site in subunit I. Thus, the phospholipid cluster seems to serve as an O_2 pool for the O_2 reduction site. The cleft is covered with the carboxyl terminal of subunit VIa, possibly to prevent the phospholipids from dissociating from the cleft. In the bacterial enzyme which does not contain subunit VIa, the phospholipids may not be completely trapped in the cleft so that only one is detectable in the crystal structure (Iwata *et al.*, 1995).

Subunits VIa and VIb stabilize the dimer state. The amino terminal moiety in the fully extended conformation is in contact with helices VII and VIII of subunit I of the other monomer (Fig. 1B). The carboxyl terminal is fixed on subunit III as described above. Subunit VIb, which does not contain any transmembrane helix, is placed near the quasi-two-fold symmetry axis on the cytosolic surface (Fig. 1B). The segment between Cys^{39} and Cys^{53} is involved in an intermonomer contact with the corresponding segment on the other monomer. These specific contacts suggest a very stable dimer.

It has long been proposed that cardiolipin is indispensable for the enzymic activity (Robinson, 1982). Our chemical analysis (unpublished results) indicates that our crystalline enzyme preparation contains one equivalent of cardiolipin per monomer. However, no cardiolipin has been detected in the crystal structure. The space between the two monomers is large enough for placing two cardiolipin molecules, though the electron density distribution in this region is too flat to detect the phospholipid. The cardiolipins in the intermonomer space, even if they are not tightly bound, could stabilize the dimer state. Once the dimer is monomerized, a fairly large conformational change in the amino terminal moiety of subunit VIa and dissociation of the phospholipids trapped in the intermonomer space would occur to obstruct redimerization of the dissociated monomers. Thus, a dimer–monomer equilibrium suggested from a hydrodynamic analysis (Suerez *et al.*, 1984) is unlikely. Bacterial cytochrome *c* oxidase, which lacks the subunits corresponding to the nuclear coded subunits of the bovine heart enzyme, is in a monomeric state (Ostermeier *et al.*, 1995). Thus, the dimer is likely to be stabilized by the above nuclear coded subunits. Kadenbach's group has discovered that the ATP/ADP ratio affects the efficiency of proton pumping and they proposed that the nucleotide binding site is at the amino terminal region of subunit VIa (Frank and Kadenbach, 1996). Their proposal has been confirmed by the finding of a possible ADP binding site at the amino terminal region of subunit VIa in the

Fig. 1. The Cα-backbone trace of bovine heart cytochrome *c* oxidase. This enzyme is in a dimeric state. Each monomer consists of 13 different subunits. Each subunit is shown in a different color. Hemes *a* and a_3 and two copper atoms of the Cu_A site are included in red structures and red balls. (A) A view to the transmembrane surface and (B) a view from the cytosolic side.

Fig. 2. A stereoscopic drawing of Cα backbone trace for the monomer of bovine heart cytochrome *c* oxidase. Core subunits, (subunits I, II, and III) are shown by yellow thin stick models. Nuclear coded subunits with the same colors as in Fig. 1 surrounds the core subunits.

crystal structure (Tsukihara *et al.,* 1996). The ADP binding may induce a change in the interaction between subunit VIa and helices VII and VIII of subunit I. The change in this interaction could affect the function of the O_2 reduction site, since the loop between helices VII and VIII contains the two histidines which coordinate Cu_B. Thus, dimer formation could provide a control mechanism of the enzymic function.

Subunits VIa and VIb, together with subunit II, create a concave surface including part of the surface of subunit I on the cytosolic side (Fig. 2). This concave surface could accept one molecule of cytochrome *c*. On the other hand, a stable 1:1 cytochrome *c*–cytochrome *c* oxidase complex has been isolated at low ionic strength (Ferguson-Miller *et al.,* 1976). However, no cytochrome *c*–cytochrome *c* oxidase crystal has provided the electron density of cytochrome *c*. Thus, cytochrome *c* may not bind uniquely to the enzyme even in the crystal.

STRUCTURE OF METAL SITES

One of the copper sites, Cu_A, is identified by its location in the extramembrane domain of subunit II, and by the intensity of electron density with clear anomalous scattering, consistent with that of two copper atoms (Tsukihara *et al.,* 1995). The electron density distribution suggests two copper atoms bridged by two sulfur atoms of cysteines to form a square planar structure. This structure, as well as some EPR results, indicate that the Cu_A site in its fully oxidized state contains a delocalized electron between the two Cu atoms. Thus, Cu_A site serves as a one-electron reduction site, as in the case of the 2Fe–2S type iron sulfur center (Antholine *et al.,* 1992). This structure confirms the results of metal analysis, 2Fe/3Cu, by Buse's group (Steffens *et al.,* 1987).

Coordinations of the other three redox active metal sites in the crystal structure are consistent with

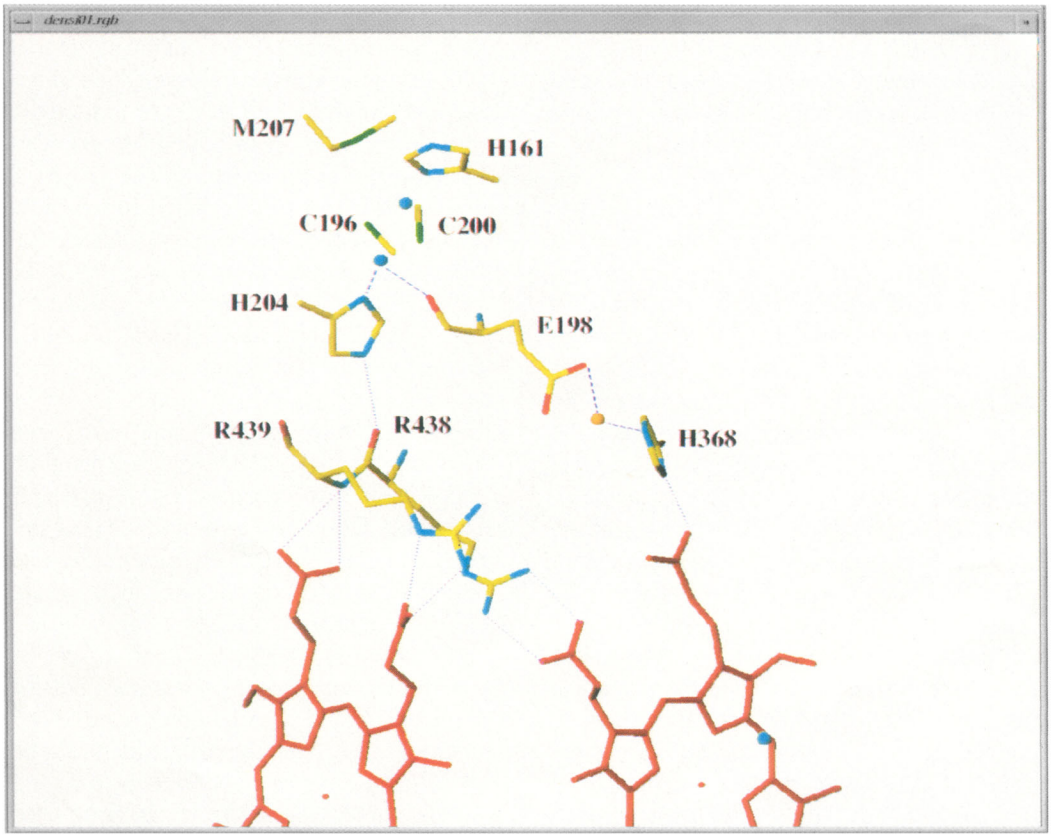

Fig. 3. Hydrogen bond network between Cu_A and hemes *a* and *a*3. Amino acids Arg^{439}, Arg^{438}, and His^{368} belong to subunit I. The other amino acids belong to subunit II. Red models with and without a small ball are hemes a_3 and *a*, respectively. Dotted lines and broken lines denote hydrogen bonds and coordination bonds, respectively. Cu_A site consists of two copper atoms (two blue balls) and six amino acids of subunit II.

the predictions by mutagenesis analysis (Hosler *et al.*, 1993; Trumpower and Gennis, 1994). Heme *a* is coordinated by His^{61} and His^{378}, heme a_3 by His^{376}, and Cu_B by His^{290}, His^{291}, and His^{240}. Three metal atoms, Fe_a, Fe_{a3}, and Cu_B, are essentially on a straight line parallel to the membrane surface. The two heme planes are essentially perpendicular to the membrane plane. The crystal structure uniquely provides the following information on the metal site structures: the distances between the metal sites, 14 Å between Fe_a and Fe_{a3}, 22 Å between Fe_{a3} and Cu_A, and 19 Å between Cu_A and Fe_a; the angle of 104° between the two heme planes; positioning of hemes (i.e., the hydroxyethyl farnesyl groups and the vinyl groups of both hemes extend toward the matrix side, while the propionates extend toward the cytosolic side), and conformation of the hydroxyethyl farnesyl groups (i.e., essentially fully extended in heme *a* and U-shaped in heme a_3). The distance between Fe_{a3} and Cu_B is 4.7 Å, and Cu_B is 1.0 Å displaced from the heme normal of Fe_{a3}. Tyr^{244} is not bound to Cu_B contrary to the conclusion from mutagenesis work (Hosler *et al.*, 1993; Trumpower and Gennis, 1994). No amino acid nor a heavy atom like sulfur or chloride is detectable in the O_2 reduction site (Tsukihara *et al.*, 1995). However, it is impossible for the electron density at 2.8 Å to disprove the presence of small atoms like oxygen or nitrogen between Fe_{a3} and Cu_B, which both have extremely high electron density.

ELECTRON TRANSFER PATHS

A hydrogen bond network between the Cu_A site and heme *a*, which includes His^{204} of subunit II, one of the Cu_A ligands, a peptide bond between Arg^{438} and Arg^{439} of subunit I, and one of the propionates of heme *a* (Fig. 3), could provide a facile electron transfer path

(Tsukihara *et al.*, 1996). On the other hand, the Cu_A site is connected by Glu^{198} of subunit II to the Mg^{2+} site. The peptide carbonyl of Glu^{198} coordinates one copper ion in the Cu_A site while its carboxyl group is one of the ligands of Mg^{2+}. Another ligand of Mg^{2+}, an imidazole of His^{368} of subunit I, forms a hydrogen-bond with one of the propionates of heme a_3. The network from Cu_A to Fe_{a3} can be a facile electron transfer path from Cu_A directly to Fe_{a3}. However, kinetic investigation of internal electron transfer has established that electron transfer from Cu_A to heme a_3 occurs via heme *a*, without any direct electron transfer from Cu_A to heme a_3 (Hill, 1994). Considering the experimental accuracy of the kinetic measurement, the direct electron transfer, if any, should be two orders of magnitude slower than that from Cu_A to heme *a*. The longer distance between Cu_A and heme a_3 (22 Å) than between Cu_A and heme *a* (19 Å) could reasonably provide such a difference in the electron transfer rate (see also Regan *et al.*, this volume).

Electron transfer between two redox active sites in the protein does not necessarily occur through a single electron transfer path. For example, heme *a* could be reduced by two electron transfer processes, namely, through a Cu_A–heme *a* path and through a Cu_A–heme a_3–heme *a* path. The redox change in each metal, not the way of transferring electrons, is physiologically relevant. However, what is the point of setting up two electron transfer paths between Cu_A and heme a_3? Furthermore, why is such a large prosthetic group as heme *a* needed for this enzyme? The roles of Cu_A and heme a_3 are obvious, as the direct electron acceptor from cytochrome *c* and O_2 binding, respectively. All enzymes in the terminal oxidase superfamily have a heme besides the O_2 binding heme (Calhoun *et al.*, 1994). The direct electron transfer path from Cu_A to heme a_3 would be enough for transferring electrons to the O_2 reduction site. The role of heme *a* may be the biggest mystery in the structure and function of cytochrome *c* oxidase.

O_2 REDUCTION MECHANISM

It has been well accepted that Cu_B, placed near the O_2 binding heme a_3, is the second electron donor for the two-electron reduction of O_2 to the peroxide level (O_2^{2-}) (Caughey *et al.*, 1976). As in the case of many metalloproteins, the conformation of metal sites in cytochrome *c* oxidase is unlikely to be influenced by the redox state. Thus, the conformation of the O_2 reduction site in the fully oxidized state suggests that O_2 is bridged between Fe_{a3}^{2+} and Cu_B^{1+} in the oxygenated form of cytochrome *c* oxidase. Then, the two-electron reduction of the bound O_2 is rate-limited by the electron transfer through one or both of the coordination bonds between the two metals and the O_2. In other words, the lifetime of the oxygenated form could be as short as a picosecond. However, resonance Raman results from three groups (Han *et al.*, 1990a; Ogura *et al.*, 1991, 1993; Varotsis *et al.*, 1993) indicate that the half-lifetime is about 0.1 msec. This result indicates a strong control mechanism for electron transfer to the bound O_2.

In the fully oxidized state, Cu_B^{2+} has only three histidine ligands. The three nitrogen atoms which coordinate Cu_B^{2+} form a triangle with Fe_{a3}^{3+} on the triangle plane. The conformation of the Cu_B site in the fully reduced state is likely to be essentially identical to the one in the fully oxidized state. Such a triangular planar Cu^{1+} compound is usually extremely stable (Cotton and Wilkinson, 1980). In other words, Cu_B^{1+} may be a poor electron donor. Also it does not readily accept any extra ligand. On the other hand, Tyr^{244} is located so close to Fe_{a3} that the distal side of O_2 bound to Fe_{a3} could form a hydrogen bond to the tyrosine-OH group. As described below, Tyr^{244} is connected to Lys^{265}, which is exposed to bulk water on the matrix side with a hydrogen bond network (Tsukihara *et al.*, 1996). Thus, Tyr^{244} can take up protons from the matrix side. Thus, this network could serve as a scalar proton transfer path.

Heme *a* is located close to heme a_3. The shortest distance between the two hemes is about 4 Å (Tsukihara *et al.*, 1995). The fifth ligand of heme a_3 is only one amino acid residue apart from one of the ligands of heme *a* in the amino acid sequence. Both features suggest facile electron transfer from heme *a* to heme a_3. Actually, resonance Raman evidence (Han *et al.*, 1990b), as well as a recent report on the absorption spectral change (Verkhovsky *et al.*, 1994), indicate that O_2 reduction is rate-limited by oxidation of heme *a*. Then, the second electron to produce peroxide could be from heme *a* and not from Cu_B.

Furthermore, the possible coordination structure of Cu_B^{1+} described above suggests that Cu_B^{1+} does not readily coordinate the distal oxygen atom of O_2 bound at Fe_{a3}. In other words, O_2 bound at Fe_{a3}^{2+} is likely to be more stable when hydrogen-bonded to Tyr^{244} than when bridged between Fe_{a3} and Cu_B. Then, O_2 bound at Fe_{a3}, when hydrogen bonded with Tyr^{244}, is reduced to peroxide by the two electrons from hemes *a* and

a_3. The rate of O_2 reduction by this process could be consistent with the lifetime of the oxygenated form determined by resonance Raman spectroscopy. The hydroperoxo intermediate, Fe^{3+}_{a3}–O–O–H, is likely to be too unstable, especially in the presence of a proton donor (i.e., Tyr^{244}), to detect during the enzymic reaction.

POSSIBLE PROTON TRANSFER PATHS

This enzyme has to transfer protons through the hydrophobic protein moiety for the two purposes, for making waters and for pumping protons from the matrix side to the cytosolic side. Possible pathways of proton transfer in the hydrophobic moiety of the protein are hydrogen bonds formed between amino acid side chains, fixed waters, and other constituents. The crystal structure shows many fairly large cavities without any electron density. Randomly oriented or mobile waters which can transfer protons are likely to be in these spaces. In some points in the transmembrane domain of the enzyme, a pair of hydrogen bond-forming amino acids are placed too far apart from each other to form a hydrogen bond, but it has small spaces to allow conformational changes in the side chains without any movement of the peptide backbone to create a new hydrogen bond. A *possible hydrogen bond structure* in this paper denotes such an arrangement of a pair of amino acids. Such a conformational change could be induced by changes in redox or ligand binding states in the metal sites.

Careful examination of the crystal structure has identified three hydrogen bond networks which involve the above three kinds of structures (Tsukihara *et al.*, 1996). Each network contains at least one *possible hydrogen bond structure.* In other words, each network has at least one disconnection point. For proton pumping, at any stable oxidation state or ligand binding state, the hydrogen bond network has to be disconnected at a certain point. The proton gradient would be discharged through a hydrogen bond network without interruption.

One of the networks connects Lys^{265} at the matrix surface to Tyr^{244} at the O_2 reduction site. Thus, it could be a channel for scalar protons (protons for making water). The presence of a *possible hydrogen bond structure* in the network indicates that the scalar proton transfer is also tightly controlled by the O_2 reduction process. The other two networks in subunit I are extended from the matrix side to the cytosolic side without direct involvement of any redox metal center. One of these is located between helices II and IV, and the other between helices XI and XII. It should be noted that if a large conformational change involving the peptide backbone is induced by change in the redox state, networks other than the above three may be identified. Furthermore, for elucidation of the mechanism of unidirectional transport of protons, it is indispensable to detect the redox-coupled conformational changes which induce pK and accessibility changes of a protonatable group. Studies are now under way for solving the structure of the fully reduced form of the enzymes at high resolution.

Recently the Cu_B site has been proposed as the site for coupling proton pumping with O_2 reduction (Wikström *et al.*, 1994; see also Wikström *et al.*, this volume). One of the key structures for this coupling mechanism (histidine cycle) is the mobility of one of the histidines coordinated to Cu_B depending on the oxidation and ligand binding states of the O_2 reduction site. Mobility of a histidine imidazole has been proposed from the crystal structure of bacterial cytochrome oxidase in the azide-bound fully oxidized state (Iwata *et al.*, 1995). The histidine imidazole at the pumping site has to have a structure which keeps the protons on the imidazole completely away from the O_2 reduction intermediate bound at Fe_{a3}, since, otherwise, the protons to be pumped will be trapped by the intermediate and will be incorporated into H_2O, as has been suggested (Williams, 1995, Wikström *et al.*, 1994). The high affinity of the O_2 reduction intermediates to protons requires an extremely effective proton insulation. However, no such structure is detectable in the O_2 reduction site of bovine heart cytochrome *c* oxidase (Tsukihara *et al.*, 1995).

ACKNOWLEDGMENT

This work was supported in part by Grants-in-Aid for Scientific Research on Priority Area (Bioinorganic Chemistry and Cell Energetics to S.Y., and No. 06276102 and No 05244102 to T. Tsukihara), Grants-in-Aid for Scientific Research (No. 06558102 to T. Tsukihara) from the Ministry of Education and Culture of Japan, and Grant-in-Aid for "Research for the Future" Program from the Japan Society for the Promotion of Science (JSPS-RFTF96L00503 to T. Tsukihara) and was done with the approval of the Photon Factory Advisory Committee, the National Laboratory for High Energy Physics, Japan (Proposal No. 91-050 and 94G-

041). We thank N. Sakabe, A. Nakagawa, N. Watanabe, and S. Ikemizu for their expert help with data collection with the Weissenberg camera and synchrotron radiation. T. Tsukihara and S.Y. are members of the TARA project of Tsukuba University.

REFERENCES

Antholine, W. E., Kastran, D. H. W., Steffens, G. C. M., Zumft, W. G., and Kröneck P. H. M. (1992). *Eur. J. Biochem.* **209**, 875–888.

Calhoun, M. W., Thomas, J. W., and Gennis, R. B. (1994). *Trends Biochem. Sci.* **19**, 325–330.

Capaldi, R. A. (1990). Annu. Rev. Biochem **59**, 569–596.

Caughey, W. S., Wallace, W. A., Volpe, J. A., and Yoshikawa, S. (1976). In *The Enzymes* (Boyer, P. D., ed.), Academic Press, New York, Vol. 13, pp. 299–344.

Chotia, C., Levitt, M., and Richardson, D. (1977). *Proc. Natl. Acad. Sci. USA* **74**, 4130–4135.

Cotton, F. A., and Wilkinson, G. (1980). In *Advanced Inorganic Chemistry*, Wiley, New York, pp. 798–821.

Einarsdottir, O., and Caughey, W. S. (1985). *Biochem. Biophys. Res. Commun.* **129**, 840–847.

Ferguson-Miller, S., Brantigan, D. L., and Margoliash, E. (1976). *J. Biol. Chem.* **251**, 1104–1115.

Frank, V., and Kadenbach, B. (1996). *FEBS Lett.* **382**, 121–124.

Han, S., Ching, Y. -C., and Rousseau, D. L. (1990a). *Biochemistry* **29**, 1380–1384.

Han, S., Ching, Y. -C., and Rousseau, D. L. (1990b). *Proc. Natl. Acad. Sci. USA* **87**, 8408–8412.

Hendler, R. W., Pardhasaradhi, K., Reynafarje, B., and Ludwig, B. (1991). *Biophys. J.* **60**, 415–423.

Hill, B. C. (1994). *J. Biol. Chem.* **269**, 2419–2425.

Hosler, J. P., Ferguson-Miller, S., Calhoun, M. W., Thomas, J. W., Hill, J., Lemiex, L., Ma, J., Georgiou, C., Fetter, J., Shapleigh, J., Tecklenburg, M. M. J., Babcock, G. T., and Gennis, R. B. (1993). *J. Bioenerg. Biomembr.* **25**, 121–135.

Iwata, S., Ostermeier, C., Ludwig, B., and Michel, H. (1995). *Nature* **376**, 660–669.

Kadenbach, B., Ungibarer, U., Jaraush, J., Buge, U., and Kuhn-Neutwig, L. (1983). *Trends. Biochem. Sci.* **8**, 398–400.

Malmström, B. G. (1990). *Chem. Rev.* **90**, 1247–1260.

Ogura, T., Takahashi, S., Shinzawa-Itoh, K., Yoshikawa, S., and Kitagawa, T. (1991). *Bull. Chem. Soc. Jpn.* **64**, 2901–2907.

Ogura, T., Takahashi, S., Hirota, S., Shinzawa-Itoh, K., Yoshikawa, S., Appelman, E. H., and Kitagawa, T. (1993). *J. Am. Chem. Soc.* **115**, 8527–8536.

Ostermeier, C., Iwata, S., Ludwig, B., and Michel, H. (1995). *Nature Struct. Biol.* **2**, 842–846.

Robinson N. C. (1982). *Biochemistry* **21**, 184–188.

Steffens, G. C. M., Biewald, R., and Buse, G. (1987). *Eur. J. Biochem.* **164**, 295–300.

Suerez, D. M., Revzin, A., Narlock, R., Kempmer, E. S., Thompson, D. A., and Ferguson-Miller, S. (1984). *J. Biol. Chem.* **259**, 13791–13799.

Tsukihara, T., Aoyama, H., Yamashita, E., Tomizaki, T., Yamaguchi, H., Shinzawa-Itoh, K., Nakashima, R., Yaono, R., Yoshikawa, S. (1995). *Science* **269**, 1069–1074.

Tsukihara, T., Aoyama, H., Yamashita, E., Tomizaki, T., Yamaguchi, H., Shinzawa-Itoh, K., Nakashima, R., Yaono, R., and Yoshikawa, S. (1996). *Science* **272**, 1136–1144.

Trumpower, B. L., and Gennis, R. B., (1994). *Annu. Rev. Biochem.* **63**, 675–716.

Varotsis, C., Zhang, Y., Appelman, E. H., and Babcock, G. T.(1993). *Proc. Natl. Acad, Sci. USA* **90**, 237–241.

Verkhovsky, M. I., Morgan, J. E., and Wikström, M. (1994). Biochemistry **33**, 3079–3086.

Wikström, M., Bogachev, A., Finel, M., Morgan, J. E., Puustinen, A., Raitio, M., Verkhovskaya, M., and Verkhovsky M. I. (1994). *Biochim. Biophys. Acta* **1187**, 106–111.

Williams, R. J. P. (1995). *Nature* **376**, 643.